

A facile and benign synthesis of binuclear ruthenium(I) “sawhorse” complexes

Christopher M. Kepert,^a Glen B. Deacon,^a Leone Spiccia,^{*a} Gary D. Fallon,^a Brian W. Skelton^b and Allan H. White^b

^a Centre for Green Chemistry and Department of Chemistry, PO Box 23, Monash University, Victoria 3800, Australia. E-mail: leone.spiccia@sci.monash.edu.au

^b Department of Physical and Inorganic Chemistry, University of Western Australia, Nedlands, Western Australia 6907, Australia

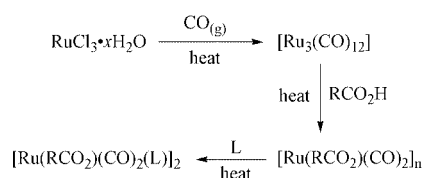
Received 23rd March 2000, Accepted 21st June 2000

Published on the Web 25th July 2000

Polymeric dicarbonyldichlororuthenium(II) $[\text{Ru}(\text{CO})_2\text{Cl}_2]_n$ is reduced by reaction with carboxylate salts ($\text{RCO}_2^- \text{Na}^+$) in alcoholic suspension. Dimeric ruthenium(I) “sawhorse” complexes $[\text{Ru}(\text{RCO}_2)(\text{CO})_2\text{L}]_2$ ($\text{R} = \text{Me}, \text{Et}, \text{Bu}^t, \text{Ph}$) are formed on the addition of a monodentate ligand, L [$\text{L} = \text{pyridine (py)}$ or 3-methylpyridine (Mepy)]. Characterisation of $[\text{Ru}(\text{MeCO}_2)(\text{CO})_2(\text{py})]_2$, $[\text{Ru}(\text{MeCO}_2)(\text{CO})_2(\text{Mepy})]_2$, $[\text{Ru}(\text{EtCO}_2)(\text{CO})_2(\text{py})]_2$, $[\text{Ru}(\text{Bu}^t\text{CO}_2)(\text{CO})_2(\text{py})]_2$ and $[\text{Ru}(\text{PhCO}_2)(\text{CO})_2(\text{py})]_2$ by IR and ^1H NMR spectroscopy is reported. Structural elucidation by single crystal X-ray diffraction was achieved in each case revealing a dicarboxylate bridged diruthenium(I) complex with cisoid carbonyls and pyridine ligands approximately collinear with the ruthenium–ruthenium bond.

The “sawhorse” di- μ -carboxylatotetracarboxyldiruthenium(I) complexes ($[\text{Ru}(\text{RCO}_2)(\text{CO})_2\text{L}]_2$) have been studied for a variety of reasons, apart from intrinsic interest. One example has been the utilisation of the bis(pyridine) adduct ($\text{L} = \text{py}$, $\text{R} = \text{Me}$) in the formulation of a dipole–dipole coupling model for application in the analysis of the IR spectra of dinuclear metal carbonyl complexes.¹ Much of the interest surrounding these compounds, however, may be attributed to their ability to catalyse a variety of organic transformations. Phosphine adducts of the ruthenium(I) dimeric species have demonstrated activity as hydrogenation catalysts in the conversion of dimethyl oxalate to methyl glycolate and ethylene glycol.² Likewise, catalytic hydrogenation and hydroformylation of alkenes, ketones and carboxylates have also been investigated.³ This has led to attempts to correlate structural features with catalytic properties. The structures of several analogous unidentate phosphine complexes, $[\text{Ru}(\mu\text{-MeCO}_2)(\text{CO})_2(\text{PBu}^n_3)]_2$,³ $[\text{Ru}(\mu\text{-RCO}_2)(\text{CO})_2(\text{PBu}^t_3)]_2$ ($\text{R} = \text{Me}, \text{Pr}^n$),^{3,4} $[\text{Ru}(\mu\text{-MeCO}_2)(\text{CO})_2(\text{PPr}^i_3)]_2$ ³ and $[\text{Ru}(\mu\text{-MeCO}_2)(\text{CO})_2(\text{Bu}^t_2\text{PH})]_2$ ⁵ have been determined by X-ray diffraction techniques. Additionally, use of bidentate phosphines, arsines and thioethers have resulted in the preparation of a plethora of ruthenium(I) polymers in which dimeric tetracarbonyl units are linked by axial ligation.⁶

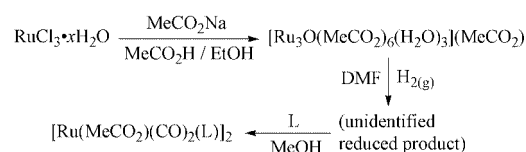
The synthesis of complexes incorporating the typical bis-(μ -carboxylate)tetracarboxyldiruthenium(I) unit have generally been based on the reaction of dodecacarbonyltriruthenium with neat carboxylic acids for prolonged periods (6–12 h) at high temperature.⁷ The products were subsequently reacted with a series of unidentate ligands to yield a class of dimeric compounds of formula $[\text{Ru}(\mu\text{-RCO}_2)(\text{CO})_2(\text{L})]_2$. The procedure is summarised in Scheme 1. The high cost of ruthenium



Scheme 1 The most extensively used synthetic methodology for $[\text{Ru}(\text{RCO}_2)(\text{CO})_2(\text{L})]_2$.

dodecacarbonyl and the difficulties encountered in their total synthesis from ruthenium trichloride have been major factors restricting the application of these complexes.

An alternative but less extensively employed procedure has entailed the reduction of μ_3 -oxo-triruthenium(III) acetate.⁸ The process is summarised in Scheme 2. Solvated with dimethyl-



Scheme 2 A further synthetic procedure affording $[\text{Ru}(\text{MeCO}_2)(\text{CO})_2(\text{L})]_2$.

formamide, this complex exists as a monovalent cation. Reduction with H_2 afforded a brown residue, which was reacted with various unidentate donors in purified deoxygenated methanol to afford the complexes $[\text{Ru}(\text{RCO}_2)(\text{CO})_2(\text{L})]_2$.⁸ In addition to difficulties attributable to the air-sensitive nature of some intermediates, reported yields were low and mixtures of products obtained.⁸

We report here a benign and efficient procedure for the synthesis of di- μ -carboxylatotetracarboxyldiruthenium(I) complexes. This novel synthetic route is based upon the facile reduction of the readily prepared dicarbonyldichlororuthenium(II) polymer⁹ in methanolic suspension in the presence of carboxylates. It provides a convenient general procedure for the formation of tetracarboxyldi- μ -carboxylatodiruthenium(I) complexes. Not only is $\text{RuCl}_3 \cdot x\text{H}_2\text{O}$ less than one fifth of the cost of $[\text{Ru}_3(\text{CO})_{12}]$, but the synthesis of the latter from the trichloride (autoclave, medium pressure)¹⁰ is much more demanding than that of $[\text{Ru}(\text{CO})_2\text{Cl}_2]_n$ ($\text{RuCl}_3 \cdot x\text{H}_2\text{O}$ with refluxing formic acid).⁹

Results and discussion

The IR spectrum of the precipitate resulting from the addition of pyridine to a boiling solution of $[\text{Ru}(\text{CO})_2\text{Cl}_2]_n$ and sodium acetate revealed at least three strong, easily discernible carbonyl

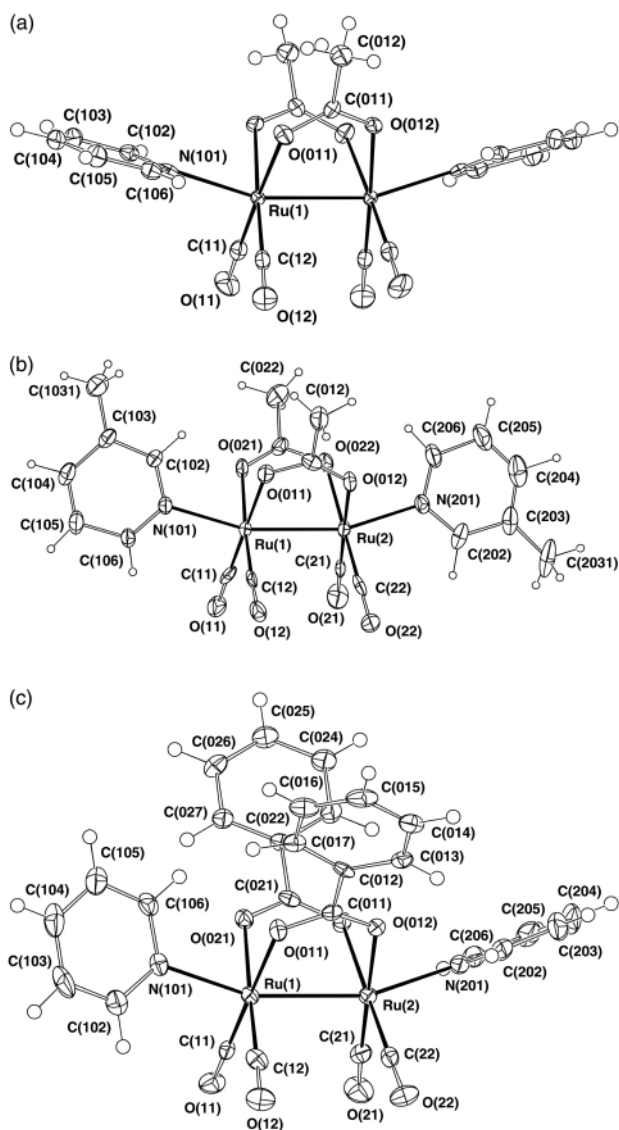


Fig. 1 Projections of representative arrays of the $[\text{Ru}(\text{RCO}_2)(\text{CO})_2\text{L}]_2$ systems: (a) $\text{R} = \text{Me}$, $\text{L} = \text{py}$, showing the $2 \times \text{flat}$ ($N\text{-base}$) $_2$ disposition; (b) $\text{R} = \text{Me}$, $\text{L} = \text{Mepy}$, (molecule 1; the other molecule is similar) showing the $2 \times \text{upright}$ ($N\text{-base}$) $_2$ disposition of the nitrogen bases; (c) $\text{R} = \text{Ph}$, $\text{L} = \text{py}$, showing the $1 \times \text{flat}$, $1 \times \text{upright}$ ($N\text{-base}$) $_2$ disposition.

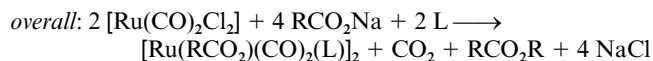
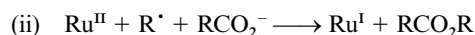
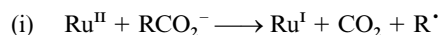
stretching frequencies. This implied the presence of more than two carbonyl ligands in either a *cis* or *fac* orientation. The ^1H NMR spectrum indicated the presence of pyridine and acetate ligands in a 1 : 1 ratio. The composition $\text{Ru}(\text{MeCO}_2)(\text{CO})_2(\text{py})$ was consistent with microanalyses, indicative of reduction of $\text{Ru}(\text{II})$ to $\text{Ru}(\text{I})$. A monomeric composition, however, is inconsistent with the IR spectrum. The $\nu(\text{CO})$ values (Nujol) 2020, 1962, 1930 cm^{-1} ; correspond to those reported⁷ for $[\text{Ru}(\text{MeCO}_2)(\text{CO})_2(\text{py})]_2$.

An X-ray diffraction study confirmed the product to be a dimeric $\text{Ru}(\text{I})$ complex ($[\text{Ru}(\text{MeCO}_2)(\text{CO})_2(\text{py})]_2$) with four *cis*-oid carbonyl and two $\mu\text{-O, O'}$ -acetate ligands in a "sawhorse" configuration [Fig. 1(a)] capped by pyridine in a position such that the ligated imine nitrogens approach the axis of the $\text{Ru}\text{--}\text{Ru}$ bond. A detailed description of this and the related structures of $[\text{Ru}(\text{MeCO}_2)(\text{CO})_2(\text{Mepy})]_2$, $[\text{Ru}(\text{EtCO}_2)(\text{CO})_2(\text{py})]_2$, $[\text{Ru}(\text{Bu}^t\text{CO}_2)(\text{CO})_2(\text{py})]_2$ and $[\text{Ru}(\text{PhCO}_2)(\text{CO})_2(\text{py})]_2$ (formed by analogous reactions with propanoate, pivalate and benzoate salts) is provided later (see Crystallography section). Reduction of ruthenium(II) was not expected under the conditions of these reactions, which were initially investigated as synthetic routes to $[\text{Ru}(\text{RCO}_2)_2(\text{CO})_2\text{L}]_2$ complexes. The presence of a large excess of a hard donor ligand and the exposure of the reaction

mixture to air are not usual conditions for the reduction of ruthenium(II).

Since the synthesis was also carried out under an atmosphere of nitrogen the possibility of reduction by methanol and concomitant oxidation to formate was excluded, as this requires dioxygen. Successful replacement of methanol solvent by the poor reductant Bu^tOH provided further evidence against the facilitation of Ru^{II} reduction by the alcohol solvent. Disproportionation to produce Ru^{I} and Ru^{III} was ruled out since there was no evidence of Ru^{III} species in the electrospray mass spectra of reaction mixtures containing methanol, MeCO_2Na and $[\text{Ru}(\text{CO})_2\text{Cl}_2]_n$. This possibility can also be discounted since the yields of Ru^{I} dimers were in some cases in excess of fifty percent. Furthermore, the reaction mixtures showed no change in colour, which could be associated with Ru^{III} complexes.

Carbon dioxide was evolved during the reaction, but was not formed when either the ruthenium polymer or sodium acetate was heated alone under the reaction conditions. Coordinated carbonyls are unlikely to be the source of carbon dioxide since similar yields of $[\text{Ru}(\text{MeCO}_2)(\text{CO})_2(\text{py})]_2$ were obtained from reactions under nitrogen and in air (an oxygen source for CO oxidation). Further, similar yields were obtained from comparable reactions under CO and Ar, whereas a higher yield would have been expected for the former if coordinated carbonyls were the source of CO_2 . Careful work-up of the reaction mixture indicated that the only ruthenium containing product detectable besides $[\text{Ru}(\text{MeCO}_2)(\text{CO})_2(\text{py})]_2$ was the known $\text{Ru}(\text{II})$ complex, $[\text{Ru}(\text{MeCO}_2)_2(\text{CO})_2(\text{py})_2]$,¹¹ which was present in trace amounts. Accordingly coordinated carbonyl ligands appear to be conserved. Thus, the acetate groups appear to be the source of CO_2 . Detection of carbon dioxide equivalent to 110% (molar basis) of the isolated dimer indicated that a two-electron oxidation of the acetate was likely. Metal-ion oxidation of carboxylates is well established.¹² In addition to the initial oxidative decomposition of the carboxylate to an alkyl radical and CO_2 , further reduction of ruthenium(II) may be facilitated by reaction of the resultant radicals to form esters, ethers or alkenes which are established products of carboxylate oxidation.¹³ Determination of carbon dioxide from the reaction of $[\text{Ru}(\text{CO})_2\text{Cl}_2]_n$ with sodium benzoate (PhCO_2Na) under comparable conditions established a similar stoichiometry. The amount of CO_2 detected compared with the product $\{[\text{Ru}(\text{PhCO}_2)(\text{CO})_2(\text{py})]_2\}$ was also 110%. Again, the formation of ruthenium dimers and CO_2 in near equimolar amounts suggests that a two-electron reduction of carboxylate occurs, as exemplified by the following sequence of reactions; for convenience the



dicarbonyldichlororuthenium(II) polymer has been treated as a monomer in yield calculations.

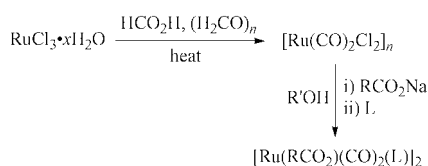
Negative electrospray mass spectroscopy of solutions formed by the simultaneous dissolution of $[\text{Ru}(\text{CO})_2\text{Cl}_2]_n$ and MeCO_2Na in methanol and by the dissolution of $[\text{Ru}(\text{CO})_2\text{Cl}_2]_n$ in methanol followed by the addition of MeCO_2Na gave similar results. Both contained major peaks at m/z 498–513 $\{[\text{Ru}_2(\text{CO})_4(\text{MeCO}_2)(\text{MeO})_2\text{Cl}_2]^- \}$, 523–535 $\{[\text{Ru}_2(\text{CO})_4(\text{MeCO}_2)_2(\text{MeO})_2\text{Cl}]^- \}$ and 547–559 $\{[\text{Ru}_2(\text{CO})_4(\text{MeCO}_2)_3(\text{MeO})_2]^- \}$. These are not present in the spectrum of a solution formed by dissolving $[\text{Ru}(\text{CO})_2\text{Cl}_2]_n$ in methanol. This indicates that the formation of the species responsible for these peaks is not

Table 1 Assignments of the ^1H NMR spectra of $[\text{Ru}(\text{RCO}_2)(\text{CO})_2(\text{L})]_2$

R, L	H2, H6	H3, H5	H4	Alkyl/phenyl
Me, py	8.74	7.43	7.83	2.06
Me, Mepy	8.56 H2 8.55 H6	7.32 H5 2.42 CH_3	7.63	2.06
Et, py	8.75	7.43	7.83	2.29 CH_2 1.05 CH_3
Bu ^t , py	8.74	7.41	7.82	1.05
Ph, py	8.93	7.53	7.92	7.85 <i>o</i> -H 7.27 <i>m</i> -H 7.39 <i>p</i> -H

dependent upon the polymer structure and that the polymer structure is likely to “break up” prior to the reduction of the metal centre.

Combinations of reagents other than acetate and pyridine have been examined in order to establish the generality of this reaction. Addition of appropriate N-pyridine bases (L) to solutions containing $[\text{Ru}(\text{CO})_2\text{Cl}_2]_n$ and various carboxylate salts (RCO_2Na) resulted in the rapid formation of a bright yellow precipitate which when recrystallised from CH_2Cl_2 afforded crystalline samples of $[\text{Ru}(\text{RCO}_2)(\text{CO})_2(\text{L})]_2$ complexes (R = Me, L = py, Mepy; R = Et, Bu^t, Ph, L = py). The microanalyses, IR and NMR spectra for all the products were consistent with their proposed formulation. The synthesis of complexes $[\text{Ru}(\text{RCO}_2)(\text{CO})_2(\text{L})]_2$ is represented in Scheme 3.

**Scheme 3** The novel and facile synthesis of the ruthenium(II) “sawhorse” dimers.

Spectroscopy

Assignments of the ^1H NMR spectra of the pyridine complexes are reported in Table 1. ^1H NMR spectra of $[\text{Ru}(\text{MeCO}_2)(\text{CO})_2(\text{py})]_2$ and $[\text{Ru}(\text{MeCO}_2)(\text{CO})_2(\text{Mepy})]_2$ reflected the symmetry of the complexes. The positions of the pyridine resonances were typical, with very little variation among the four pyridine complexes, and only slight changes in the Mepy complex due to the inductive effects of the methyl substituent. The spectra of $[\text{Ru}(\text{EtCO}_2)(\text{CO})_2(\text{py})]_2$ and to a greater extent $[\text{Ru}(\text{Bu}^t\text{CO}_2)(\text{CO})_2(\text{py})]_2$ exhibited broadened signals, hence coupling constants could not be determined. Steric interactions between the pyridine rings and the propanoate or the bulkier pivalate groups may constitute a barrier to rotation which was not completely overcome at room temperature. This may engender slight inequivalence of protons on the two pyridine rings which would otherwise experience identical environments.

IR spectroscopy revealed intense bands in the region associated with absorptions due to carbonyl ligands in patterns consistent with previous reports of these and similar compounds.^{1,4,7} Assignment of $\nu_{\text{as}}(\text{CO}_2)$ can be made to absorption bands occurring within the range 1556–1574 cm^{-1} . The identification of the symmetrical stretching mode (ν_{s}) was not as straightforward, owing to the presence of a number of bands in the region. Peaks in the vicinity of 1440–1450 cm^{-1} are the most likely candidates in complexes incorporating alkyl carboxylate bridges, although identification of $\nu_{\text{s}}(\text{CO}_2)$ could not be made for $[\text{Ru}(\text{EtCO}_2)(\text{CO})_2(\text{py})]_2$. The average gap between the $\nu_{\text{as}}(\text{CO}_2)$ and $\nu_{\text{s}}(\text{CO}_2)$ vibrational modes corresponds to *ca.* 125 cm^{-1} in agreement with previously reported spectra for these types of complexes,⁷ and falls within the region reported

for other μ -*O,O'*-carboxylate complexes.^{14,15} This family of compounds constitutes a typical example where the energy separation between the symmetric and antisymmetric stretching modes for a bridging carboxylate is smaller than for that of its ionic counterpart (*e.g.*, *ca.* 164 cm^{-1} for ionic acetate).¹⁴

Crystallography

Each of the complexes gave high quality crystals upon recrystallisation (albeit twinned in a number of cases), and consequently X-ray structural characterisation was undertaken. ORTEP¹⁶ representations of the molecular structures of $[\text{Ru}(\text{MeCO}_2)(\text{CO})_2(\text{py})]_2$, $[\text{Ru}(\text{MeCO}_2)(\text{CO})_2(\text{Mepy})]_2$, and $[\text{Ru}(\text{PhCO}_2)(\text{CO})_2(\text{py})]_2$ are displayed in Fig. 1. Table 2 summarises the geometric features of the ruthenium centres. The five complexes are of analogous composition and structure, and are identical in terms of stoichiometry (all unsolvated), connectivity and stereochemistry. In the structures of the binuclear complexes, $[(\text{L})(\text{OC})_2\text{Ru}(\mu\text{-O-CR-O'})_2\text{Ru}(\text{CO})_2(\text{L})]$, the pair of ruthenium atoms are six-coordinate with similar coordination environments. The Lewis-base donor lies approximately collinear with the ruthenium–ruthenium bond (which may be regarded as defining an axis) and the pairs of carbonyl and μ -*O,O'*-carboxylate donors are mutually *cis* in the plane (containing the Ru–O and Ru–C bonds) equatorial to that axis. The total array of the ruthenium atoms and their immediate neighbours approximates $2m$ (C_{2v}) symmetry, the two-fold axis lying normal to the Ru–Ru bond and contained in the mirror plane which passes between and relates the two carboxylate groups, and also contains the Ru–Ru bond. A second pseudo mirror plane lies normal to the Ru–Ru bond. Further from the molecular core, the symmetry may be perturbed by the relative dispositions of the carboxylate alkyl substituents, and by the relative dispositions of the aromatic rings of the axially coordinated ligands, which tend to lie within or bisected by the mirror plane. The three possible combinations observed are illustrated in Fig. 1. Despite the potential symmetry of the binuclear species, $[\text{Ru}(\text{MeCO}_2)(\text{CO})_2(\text{py})]_2$ is the only one of these molecules to conform to any crystallographic symmetry element. The binuclear unit comprises the asymmetric unit in the remainder of the complexes with the exception of $[\text{Ru}(\text{MeCO}_2)(\text{CO})_2(\text{Mepy})]_2$, in which two pseudo-symmetrically related molecules comprise the asymmetric unit in a non-centrosymmetric space group. In view of crystallographic difficulties (*e.g.*, the twinned nature of the crystals), interpretation of the geometries obtained from the determination of the structure of $[\text{Ru}(\text{MeCO}_2)(\text{CO})_2(\text{Mepy})]_2$ should be treated with appropriate circumspection. {In regard to supramolecular dispositions, it is of interest that the packing found in $[\text{Ru}(\text{MeCO}_2)(\text{CO})_2(\text{py})]_2$, $[\text{Ru}(\text{MeCO}_2)(\text{CO})_2(\text{Mepy})]_2$, $[\text{Ru}(\text{EtCO}_2)(\text{CO})_2(\text{py})]_2$ and $[\text{Ru}(\text{Bu}^t\text{CO}_2)(\text{CO})_2(\text{py})]_2$ is approximately symmetrical, *quasi*-2 approximately parallel to monoclinic *b*, and *quasi*-*m* approximately normal to *a*.}

The geometries of the five pyridine and 3-methylpyridine adducts are similar (Table 2), differing only for $[\text{Ru}(\text{Bu}^t\text{CO}_2)(\text{CO})_2(\text{py})]_2$ and $[\text{Ru}(\text{PhCO}_2)(\text{CO})_2(\text{py})]_2$ in more general features such as the dispositions of the pyridine rings, and some slight twisting of the carboxylates, perhaps in response to the different relative dispositions of *tert*-butyl substituents, whose relation appears to be determined by gearing considerations. Notwithstanding these observations, bond lengths and angles among the five compounds may be regarded as archetypal. About the ruthenium atoms, the most notable feature is the enlargement of the angles between the *cis*-carbonyl and carboxylate donors [*e.g.*, O(1)–Ru–C(2)] in response to the smaller angles between the pair of *cis*-carboxylate oxygen atoms [O(1)–Ru–O(2) angles of 93–96° resulting from O(1)–Ru–O(2) angles of *ca.* 84°], the latter persisting despite the presence of *tert*-butyl groups adjacent to each other on adjoining bridging ligands in the $[\text{Ru}(\text{Bu}^t\text{CO}_2)(\text{CO})_2(\text{py})]_2$ complex [O(1)–Ru–O(2) of 83.95(8)

Table 2 Ruthenium environments in ruthenium(II) pyridine complexes. The five vertical values in each entry are for (a) $[\text{Ru}(\text{MeCO}_2)(\text{CO})_2(\text{py})]_2$, (b) molecules i and ii of $[\text{Ru}(\text{MeCO}_2)(\text{CO})_2(3\text{-Mepy})]_2$ (two crystallographically inequivalent molecules), (c) $[\text{Ru}(\text{EtCO}_2)(\text{CO})_2(\text{py})]_2$, (d) $[\text{Ru}(\text{Bu}^t\text{CO}_2)(\text{CO})_2(\text{py})]_2$ and (e) $[\text{Ru}(\text{PhCO}_2)(\text{CO})_2(\text{py})]_2$. $r(\text{\AA})$ is the ruthenium–ligand atom distance, other entries being the angles ($^\circ$) subtended by the pertinent atoms at the head of the row and column. The two values in each entry are for Ru(1,2), except for $[\text{Ru}(\text{MeCO}_2)(\text{CO})_2(\text{py})]_2$ in which the two Ru are related by symmetry. For (b) and (e), C(1) and O(1) correspond to the lowest numbered carbon and oxygen donor atoms attached to each ruthenium of Fig. 1(b) and (c), respectively

Atom		r	C(1)	C(2)	O(1)	O(2)	N
Ru	(a)	2.672(1)	92.6(2)	96.0(2)	84.6(1)	82.6(1)	162.7(1)
	(b)i	2.678(2)	95.8(5), 96.8(5)	92.8(5), 96.4(5)	83.8(3), 84.1(3)	84.3(3), 82.9(3)	163.7(4), 162.2(4)
	(b)ii	2.678(2)	95.2(5), 95.0(6)	93.9(5), 94.0(5)	83.6(3), 84.4(3)	83.7(3), 84.2(3)	163.5(4), 164.1(4)
	(c)	2.676(1)	95.2(3), 93.9(3)	94.7(3), 95.3(3)	82.5(2), 84.2(2)	83.9(2), 82.9(2)	161.5(2), 162.7(2)
	(d)	2.6760(6)	94.7(1), 95.2(1)	93.6(1), 95.8(1)	84.06(6), 83.25(7)	84.03(5), 83.47(6)	163.73(6), 161.82(6)
	(e)	2.6780(4)	94.8(1), 96.1(1)	94.7(1), 95.4(1)	83.77(6), 84.39(6)	84.17(6), 84.16(6)	161.46(8), 161.80(8)
C(1)	(a)	1.836(6)		87.8(2)	176.6(2)	94.3(2)	99.2(2)
	(b)i	1.78(2), 1.77(2)		88.4(9), 87(1)	178.8(6), 178.9(6)	93.6(7), 94.9(8)	94.3(7), 95.2(7)
	(b)ii	1.83(2), 1.83(2)		89.7(9), 90.9(8)	176.3(8), 177.7(7)	93.0(8), 93.0(7)	97.3(6), 96.9(7)
	(c)	1.840(8), 1.834(7)		88.5(4), 89.4(3)	177.3(4), 176.5(3)	94.4(3), 92.5(3)	98.4(4), 97.5(3)
	(d)	1.836(3), 1.830(3)		90.3(1), 87.9(1)	177.3(1), 177.6(1)	93.5(1), 93.3(1)	96.0(1), 97.0(1)
	(e)	1.834(4), 1.826(4)		88.3(2), 87.4(2)	177.4(1), 179.4(2)	93.7(1), 94.6(1)	100.2(1), 96.4(1)
C(2)	(a)	1.846(6)			94.4(2)	177.5(2)	96.9(2)
	(b)i	1.78(2), 1.81(2)			92.7(7), 93.2(7)	176.7(7), 177.7(7)	100.2(6), 97.2(7)
	(b)ii	1.84(2), 1.83(2)			93.9(8), 91.4(7)	176.5(8), 175.9(7)	97.0(7), 96.3(6)
	(c)	1.834(9), 1.829(7)			93.1(3), 93.7(3)	176.9(3), 177.5(3)	98.2(4), 97.8(3)
	(d)	1.826(3), 1.826(3)			92.3(1), 94.0(1)	175.7(1), 178.6(1)	98.5(1), 98.1(1)
	(e)	1.824(4), 1.833(4)			94.0(1), 92.9(1)	177.8(1), 178.1(1)	96.7(1), 98.4(1)
O(1)	(a)	2.133(4)				83.4(1)	83.0(1)
	(b)i	2.10(1), 2.12(1)				85.3(5), 84.6(5)	85.9(5), 83.8(5)
	(b)ii	2.10(1), 2.12(1)				83.4(5), 84.8(5)	83.2(5), 83.3(5)
	(c)	2.114(5), 2.118(5)				83.9(2), 84.3(2)	83.5(2), 83.7(2)
	(d)	2.125(2), 2.117(2)				83.95(8), 84.72(9)	84.67(8), 84.1(1)
	(e)	2.118(2), 2.141(3)				84.03(8), 85.13(8)	80.9(1), 83.0(1)
O(2)	(a)	2.135(4)		θ^a 67.5(1)			84.1(1)
	(b)i	2.13(1), 2.10(1)		71(1)			82.3(5), 83.1(6)
	(b)ii	2.11(1), 2.10(1)		76(1)			84.9(5), 84.7(5)
	(c)	2.121(5), 2.121(5)		73.1(4)			82.6(2), 83.6(2)
	(d)	2.121(2), 2.107(2)		70.8(1)			83.15(8), 82.43(9)
	(e)	2.134(2), 2.122(2)		84.9(2)			84.0(1), 81.71(9)
N	(a)	2.197(4)					
	(b)i	2.25(1), 2.21(2)					
	(b)ii	2.24(1), 2.21(1)					
	(c)	2.235(7), 2.224(7)					
	(d)	2.225(2), 2.224(3)					
	(e)	2.224(3), 2.195(3)					

^a θ ($^\circ$) is the dihedral angle between the two carboxylate C_2O_2 planes.

and 84.72(9) $^\circ$]. Ruthenium–nitrogen and –oxygen bonds appear unperturbed by substituent effects, and variation in ruthenium–ruthenium and –carbon bonds by any consequent *trans*-influence is limited in extent. Ruthenium–carbonyl distances vary little, being typically around 1.83 Å, while Ru–O and Ru–N bond lengths are close to 2.12 and 2.22 Å, respectively. These values match those in a related acetone nitrile complex, $[\text{Ru}(\text{CF}_3\text{CO}_2)(\text{CO})_2(\text{NCMe})]_2$, in which the average Ru–N bond length is 2.18 Å, Ru–O is 2.133(3) Å, Ru–C is 1.83 Å, and the Ru–Ru separation is marginally larger at 2.683(1) Å.¹⁷ The deviation in the Ru–Ru bond distances in the pyridine and 3-methylpyridine complexes is insignificant, with an average separation of 2.677(1) Å. Distances in the imine complexes are consistently shorter than those reported for phosphine structural analogues $\{[\text{Ru}(\mu\text{-O}_2\text{CMe})(\text{CO})_2(\text{Pr}^t\text{PH})]_2, [\text{Ru}(\mu\text{-O}_2\text{CMe})(\text{CO})_2(\text{Bu}^t\text{P})]_2, [\text{Ru}(\mu\text{-O}_2\text{CMe})(\text{CO})_2(\text{Bu}^t\text{P})]_2, [\text{Ru}(\mu\text{-O}_2\text{CMe})(\text{CO})_2(\text{Bu}^t\text{PH})]_2$ and $[\text{Ru}(\mu\text{-O}_2\text{CPr}^n)(\text{CO})_2(\text{Bu}^t\text{P})]_2\}$, for which the average inter-ruthenium distance is 2.735(2) Å.³ Conversely, distances found in complexes with aqua and carbonyl or carboxylic acid ligands occupying positions approximately *trans* to the Ru–Ru bond are indicative of a small but consistent increase in Ru–Ru bond order.¹⁸ Comparison of Ru–N bond distances of the dimers with those in other pyridine complexes reveal that the separ-

ations of 2.20–2.25 Å in the five Ru^{I} imine complexes are significantly longer than those observed in octahedral Ru^{II} pyridine complexes {e.g., average of 2.12(1) Å in $[\text{Ru}(\text{py})_6]^{2+}$ }.¹⁹ Apart from the larger cationic radius of Ru^{I} in comparison to Ru^{II} , this elongation may be attributed to the considerable *trans*-influence of a metal–metal bond, which probably contributes to the lability of the pyridine in such species. Substituent effects on the ruthenium–ruthenium bond length have been discussed in some detail.²⁰

The packing motifs of $[\text{Ru}(\text{MeCO}_2)(\text{CO})_2(\text{py})]_2$, $[\text{Ru}(\text{MeCO}_2)(\text{CO})_2(\text{Mepy})]_2$, $[\text{Ru}(\text{EtCO}_2)(\text{CO})_2(\text{py})]_2$ and $[\text{Ru}(\text{Bu}^t\text{CO}_2)(\text{CO})_2(\text{py})]_2$ seem to be largely determined by the packing considerations of and interactions between the pyridine moieties {e.g., an intermolecular contact of 3.566(8) Å is observed between N(101) and C(104) in the structure of $[\text{Ru}(\text{MeCO}_2)(\text{CO})_2(\text{py})]_2$ }. The introduction of a phenyl substituent in the benzoate/pyridine complex causes a perturbation of the long range chain-like order observed in $[\text{Ru}(\text{MeCO}_2)(\text{CO})_2(\text{py})]_2$ by enabling association of pairs of the dimer through π -stacking of these groups. The low intermolecular separation of 3.594(9) Å for C(105) \cdots C(105') implies the existence of such interactions between the phenyl rings.

Conclusion

The new more benign synthetic procedure reported here provides convenient access to di- μ -acetatotetracarbonylruthenium(II) complexes and should stimulate interest in the further application of such complexes. Substitution reactions involving the exchange of the pyridine ligands with monodentate and bidentate ligands, to be reported in a subsequent paper, lead to an even greater array of binuclear ruthenium(II) complexes.

Experimental

Physical measurements

IR spectra were recorded using a Perkin-Elmer 1640 FTIR spectrophotometer as Nujol mulls. ^1H NMR spectra were recorded in CDCl_3 on a Bruker AM300 spectrometer at 300 MHz. Elemental microanalyses were performed by Chemical and Micro Analytical Services (CMAS), Melbourne, Australia.

Materials and reagents

HPLC grade methanol was used in preparation of complexes. *tert*-Butyl alcohol was purified by crystallisation and dried over sodium prior to use. Sodium pivalate and sodium propanoate were prepared by reaction of the appropriate carboxylic acids with sodium carbonate in aqueous media, with the isolated salt recrystallised and dried by heating under vacuum. All other chemicals were of reagent or analytical reagent grade and were used without further purification. $[\text{Ru}(\text{CO})_2\text{Cl}_2]_n$ was synthesised according to an existing method.⁹

Syntheses

Di- μ -*O*,*O'*-acetatotetracarbonylbis(pyridine)diruthenium(II), $[\text{Ru}(\text{MeCO}_2)(\text{CO})_2(\text{py})_2]_2$. (i). $[\text{Ru}(\text{CO})_2\text{Cl}_2]_n$ (0.66 g, 2.9 mmol) was added to a solution of a large excess of sodium acetate (2.80 g, 34 mmol) in degassed methanol (75 ml). The resultant suspension was heated at a bath temperature of *ca.* 120 °C under an atmosphere of nitrogen for a period of 2.5 h, during which the reagents dissolved giving an orange solution. Introduction of pyridine (0.70 ml, 8.7 mmol) resulted in an instantaneous change of the solution to bright yellow and the rapid formation of a light yellow precipitate ensued. After 5 min continued heating, and cooling to -10 °C, $[\text{Ru}(\text{MeCO}_2)(\text{CO})_2(\text{py})_2]_2$ was isolated as a yellow microcrystalline solid, washed with ice-cold methanol (2×10 ml), and dried in air at 70 °C (yield: 0.358 g, 42%). The filtrate was evaporated to 10 ml, resulting in a precipitation of a mixture of sodium acetate and $[\text{Ru}(\text{MeCO}_2)(\text{CO})_2(\text{py})_2]_2$. Suspension of the mixture in the minimum volume of CH_2Cl_2 and subsequent filtration was repeated until the residual solid was colourless. The combined filtrate was added to methanol (5 ml). Further evaporation afforded additional $[\text{Ru}(\text{MeCO}_2)(\text{CO})_2(\text{py})_2]_2$ (yield: 0.108 g, 13%). Total yield: 0.466 g, 55%. Found: C, 36.6; H, 2.5; N, 4.7. $\text{C}_{18}\text{H}_{16}\text{N}_2\text{O}_8\text{Ru}_2$ requires C, 36.6; H, 2.7; N, 4.7%. IR ν/cm^{-1} : 2020s, 1962s, 1930s $\nu(\text{CO})$; 1600w, 1568s $\nu_{\text{as}}(\text{CO}_2)$; 1449s $\nu_{\text{s}}(\text{CO}_2)$; 1352w, 1217m, 1070m, 1040w, 1012w, 754m, 697m. δ_{H} (300 MHz, CDCl_3): 8.74 (4H, dt, $^3J = 4.7$, $^4J \approx 1.5$ Hz); 7.83 (2H, tt, $^3J = 7.6$, $^4J = 1.6$ Hz); 7.43 (4H, ddd, $^3J = 7.7$, $^3J = 4.7$, $^4J = 1.5$ Hz); 2.06 (6H, s, CH_3CO_2).

(ii) The preparation was successfully repeated in air affording a similar yield of product.

(iii) *Under a CO atmosphere.* $[\text{Ru}(\text{CO})_2\text{Cl}_2]_n$ (0.66 g, 2.9 mmol) was added to a solution of NaO_2CMe (2.80 g, 34 mmol) in 75 ml of MeOH. The mixture was purged with CO for 20 min and then refluxed for 2.5 h. The initially yellow solution rapidly changed to orange. After completion of the reaction, pyridine (0.7 ml, 8.7 mmol) was added to the hot solution causing a change to yellow and a yellow precipitate formed. After cooling to room temperature, then to -20 °C overnight, the product was collected, washed with cold MeOH and air-dried at 80 °C

(yield: 0.60 g, 70%). IR and ^1H NMR (CDCl_3) data were in agreement with those of the product from (i). A weak CO absorption at 2067 cm^{-1} was also detected and may be attributed to an impurity of $[\text{Ru}(\text{MeCO}_2)_2(\text{CO})_2(\text{py})_2]_2$,¹¹ although this was not detected by NMR spectroscopy. The filtrate was evaporated to dryness and extracted with CH_2Cl_2 (50 ml). The white residue was NaO_2CMe containing no detectable metal carbonyl species (IR). The CH_2Cl_2 extract was evaporated to an oily yellow solid and attempted recrystallisation from MeOH– H_2O gave a small amount (*ca.* 5 mg) of $[\text{Ru}(\text{MeCO}_2)(\text{CO})_2(\text{py})_2]_2$ (IR identification). The remaining material was isolated by evaporation to dryness (yield: 0.10 g) and an IR spectrum (as a CH_2Cl_2 solution) showed strong CO absorptions at 2059 and 1992 cm^{-1} consistent with the presence of predominantly $[\text{Ru}(\text{MeCO}_2)_2(\text{CO})_2(\text{py})_2]_2$.¹¹

(iv) *Under an argon atmosphere.* A similar reaction conducted under an argon atmosphere showed similar features and gave the same product (yield: 0.66 g, 77%). IR and ^1H NMR (CDCl_3) data were in agreement with those of the product from (i). The presence of a trace of $[\text{Ru}(\text{MeCO}_2)_2(\text{CO})_2(\text{py})_2]_2$ was again indicated by a shoulder on the 2020 cm^{-1} $\nu(\text{CO})$ absorption of the product. The filtrate was evaporated to dryness and extracted with CH_2Cl_2 (50 ml). The remaining white solid (NaO_2CMe) showed no $\nu(\text{CO})$ absorption in the IR spectrum. The CH_2Cl_2 solution was evaporated to an oily yellow solid (0.07 g) and an IR spectrum (as a CH_2Cl_2 solution) showed strong $\nu(\text{CO})$ absorptions at 2059, 1990 and 1964 cm^{-1} consistent with the presence of a mixture of the main product and $[\text{Ru}(\text{MeCO}_2)_2(\text{CO})_2(\text{py})_2]_2$.¹¹

(v) The repetition of (i) (above) with $[\text{Ru}(\text{CO})_2\text{Cl}_2]_n$ (0.942 g, 4.1 mmol) and sodium acetate (2.85 g, 35 mmol) in *tert*-butyl alcohol (50 ml) afforded $[\text{Ru}(\text{MeCO}_2)(\text{CO})_2(\text{py})_2]_2$, as identified by IR and ^1H NMR spectroscopy (yield: 0.658 g, 54%).

Tetracarbonyl-di- μ -*O*,*O'*-propanoatobis(pyridine)diruthenium(II), $[\text{Ru}(\text{EtCO}_2)(\text{CO})_2(\text{py})_2]_2$. Reaction of dicarbonyldichlororuthenium(II) (0.650 g, 2.85 mmol) with sodium propanoate (1.06 g, 11 mmol) as in (i) gave $[\text{Ru}(\text{EtCO}_2)(\text{CO})_2(\text{py})_2]_2$ as yellow crystals (yield: 0.362 g, 41%). Found: C, 38.7; H, 3.1; N, 4.4. $\text{C}_{20}\text{H}_{20}\text{N}_2\text{O}_8\text{Ru}_2$ requires C, 38.8; H, 3.3; N, 4.5%. IR ν/cm^{-1} : 2016s, 1957s, 1932s $\nu(\text{CO})$; 1601w, 1567s $\nu(\text{CO}_2)$; 1376m, 1303w, 1216m, 1152w, 1086w, 1069m, 1039w, 1009w, 894w, 811w, 751w, 688m. δ_{H} (300 MHz, CDCl_3): 8.75 (4H, d, $^3J = 5.0$ Hz); 7.83 (2H, t, $^3J = 7.8$ Hz); 7.43 [4H, apparent triplet (br), $^3J \approx 6.6$ Hz]; 2.29 (4H, q, $^3J = 7.6$ Hz, $\text{CO}_2\text{CH}_2\text{CH}_3$); 1.05 (6H, t, $^3J = 7.5$ Hz, $\text{CO}_2\text{CH}_2\text{CH}_3$).

Tetracarbonyl-di- μ -*O*,*O'*-pivalatobis(pyridine)diruthenium(II), $[\text{Ru}(\text{Bu}^t\text{CO}_2)(\text{CO})_2(\text{py})_2]_2$. The corresponding pivalate complex $[\text{Ru}(\text{Bu}^t\text{CO}_2)(\text{CO})_2(\text{py})_2]_2$ was prepared by (i) (above) from sodium pivalate (2.9 g, 23 mmol), which was reacted with $[\text{Ru}(\text{CO})_2\text{Cl}_2]_n$ (0.660 g, 2.89 mmol). Yield 0.497 g (0.74 mmol, 51%). Found: C, 41.5; H, 4.0; N, 4.0. $\text{C}_{24}\text{H}_{28}\text{N}_2\text{O}_8\text{Ru}_2$ requires C, 40.6; H, 4.3; N, 4.3%. IR ν/cm^{-1} : 2014s, 1958s, 1933s $\nu(\text{CO})$; 1600w, 1562s $\nu(\text{CO}_2)$; 1447s, 1419m, 1361m, 1226w, 1216m, 1152w, 1066w, 1040w, 1010w, 937w, 806w, 756m, 696m. δ_{H} (300 MHz, CDCl_3): 8.74 [4H, s (br)]; 7.82 [2H, s (br)]; 7.41 [4H, d (br), $^3J = 5.4$ Hz]; 1.05 [18H, s, $\text{C}(\text{CH}_3)_3\text{CO}_2$].

Di- μ -*O*,*O'*-benzoatotetracarbonylbis(pyridine)diruthenium(II), $[\text{Ru}(\text{PhCO}_2)(\text{CO})_2(\text{py})_2]_2$. Addition of pyridine to a solution formed by the reaction of $[\text{Ru}(\text{CO})_2\text{Cl}_2]_n$ (0.670 g, 2.9 mmol) with sodium benzoate (1.10 g, 76 mmol) according to (i) resulted in the precipitation of bright yellow $[\text{Ru}(\text{PhCO}_2)(\text{CO})_2(\text{py})_2]_2$ (yield: 0.620 g, 59%). Found: C, 48.1; H, 2.8; N, 3.9. $\text{C}_{24}\text{H}_{20}\text{N}_2\text{O}_8\text{Ru}_2$ requires C, 47.1; H, 2.8; N, 3.8%. IR ν/cm^{-1} : 2027s, 1977s, 1954s, 1911m $\nu(\text{CO})$; 1596s, 1560s, 1448s $\nu(\text{CO}_2)$; 1409s, 1215m, 1182w, 1172w, 1156w, 1068m, 1037w, 1029w, 1008w, 942w, 855w, 815w, 755m, 695s, 668m. δ_{H} (300 MHz, CDCl_3): 8.93 (4H, d, $^3J = 4.8$ Hz); 7.92 (2H, t, $^3J = 7.5$ Hz); 7.85

(4H, apparent doublet of triplets, $^3J = 6.9$, $^4J \approx 1.4$ Hz); 7.53 (4H, apparent triplet (br), $^3J \approx 6$ Hz); 7.39 (2H, tt, $^3J = 7.3$, $^4J = 1.4$ Hz); 7.27 (4H, ddm, $^3J = 7.3$, $^3J = 6.9$, $J \approx 1$ Hz).

Di- μ -O, O'-acetatotetracarboxylbis(3-methylpyridine)-diruthenium(I), [Ru(MeCO₂)(CO)₂(Mepy)]₂. Addition of 3-methylpyridine (0.70 ml) instead of pyridine to [Ru(CO)₂Cl₂]_n (0.462 g, 2.0 mmol) according to (i) resulted in the formation of [Ru(CO)₂(MeCO₂)(Mepy)]₂ as a yellow crystalline solid (yield: 0.245 g, 41%). Found: C, 38.7; H, 3.2; N, 4.5. C₂₀H₂₀N₂O₈Ru₂ requires C, 38.8; H, 3.3; N, 4.5%. IR ν /cm⁻¹: 2021s, 1960s, 1928s (br) ν (CO); 1882m (sh), 1574s, 1441s ν (CO₂); 1349m (sh), 1243w, 1197m, 1127w, 1104w, 1057m, 1023w, 814w, 792m, 697m, 650m. δ_{H} (300 MHz, CDCl₃): 8.56 (2H, s); 8.55 (2H, d, $^3J = 5.5$ Hz); 7.63 (2H, d, $^3J = 7.5$ Hz); 7.32 (2H, dd, $^3J = 7.5$, $^3J = 5.5$ Hz); 2.42 (6H, s, py-CH₃); 2.06 (6H, s, CH₃CO₂).

Carbon dioxide analysis

Detection of carbon dioxide from reactions performed under identical conditions to those outlined in the preparation of [Ru(MeCO₂)(CO)₂(py)]₂ was effected by the precipitation of barium carbonate from a saturated aqueous solution of barium hydroxide on passage of the effluent nitrogen flow from the reaction vessel. Carbon dioxide was not detected by this method when either the ruthenium polymer or the acetate salt were subjected to the same treatment, thus eliminating the possibility that carbon dioxide was inadvertently introduced into the system.

[Ru(MeCO₂)(CO)₂(py)]₂. [Ru(CO)₂Cl₂]_n [0.907 g, 4.0 mmol (monomer assumed)] and excess sodium acetate (2.5 g) in degassed methanol (75 ml) yielded BaCO₃ 0.219 g (1.11 mmol, 56%). Addition of pyridine (1.00 ml) afforded [Ru(MeCO₂)(CO)₂(py)]₂ (0.582 g, 0.99 mmol, 49%) as a yellow crystalline solid.

[Ru(PhCO₂)(CO)₂(py)]₂. Reaction of [Ru(CO)₂Cl₂]_n (0.976 g, 4.3 mmol) with an excess of sodium benzoate (3.0 g) in degassed methanol (75 ml) gave BaCO₃ 0.267 g (1.4 mmol, 56% per Ru). [Ru(PhCO₂)(CO)₂(py)]₂ (0.866 g, 1.21 mmol, 56%) precipitated upon the addition of pyridine (1.00 ml).

Structure determination

Three room-temperature single-counter four-circle diffractometer data sets were measured (graphite-monochromated Mo-K α radiation, $\lambda = 0.71073$ Å; 2θ - θ scan mode, $2\theta_{\text{max}}$ as specified, $T \approx 295$ K) in addition to one low-temperature data set ($T = 173$ K) yielding N independent reflections, N_0 with $I > 3\sigma(I)$ being considered 'observed' and used in the full-matrix least-squares refinement after Gaussian absorption correction. A fifth data set was collected at 123 K with a Kappa-Nonius CCD diffractometer, and was processed without absorption correction. Anisotropic thermal parameter forms were refined for the non-hydrogen atoms, (x , y , z , U_{iso})_H being included constrained at estimated values. Conventional residuals R , R_w on $|F|$ are quoted at convergence. Neutral atom complex scattering factors were used. Calculations were performed using either the Xtal 3.4 program system²¹ or the teXsan crystallographic package.²²

Crystal/refinement data. (a) *Pyridine/acetate adduct.* Ru₂C₁₈H₁₆N₂O₈, $M = 590.47$, monoclinic, space group $C2/c$ (no. 15), $a = 15.746(7)$, $b = 8.634(4)$, $c = 15.837(7)$ Å, $\beta = 106.42(4)^\circ$, $V = 2066(2)$ Å³, D_c ($Z = 4$) = 1.89 g cm⁻³, $F(000) = 1160$, μ_{Mo} = 15.10 cm⁻¹, $2\theta_{\text{max}} = 50.0^\circ$; $N = 1959$, $N_0 = 1567$; $R = 0.027$, $R_w = 0.034$; $n_v = 136$, $|\Delta\rho_{\text{max}}| = 0.58$ e Å⁻³.

Variata. Data were measured at 173 K. 1567 reflections with $I > 3.00\sigma(I)$ were used in a full-matrix least-squares refinement

after Lorentz-polarization and empirical absorption corrections (transmission factors 0.689₃–1.000) using the program DIFABS.²³ Structure solution was effected by use of DIRDIF94²⁴ and refined with the teXsan²² crystallographic software package.

(b) *3-Methylpyridine/acetate adduct.* C₂₀H₂₀N₂O₈Ru₂, $M = 618.5$, monoclinic, space group $P2_1$ (no. 4), $a = 11.063(7)$, $b = 15.445(5)$, $c = 15.110(4)$ Å, $\beta = 111.57(4)^\circ$, $V = 2401$ Å³, D_c ($Z = 4$) = 1.71 g cm⁻³, $F(000) = 1224$, μ_{Mo} = 13.0 cm⁻¹; specimen: 0.85 × 0.50 × 0.20 mm; $A^*_{\text{min,max}} = 1.23, 1.44$; $2\theta_{\text{max}} = 50^\circ$; $N = 4382$, $N_0 = 3456$; $R = 0.051$, $R_w = 0.058$; $n_v = 580$, $|\Delta\rho_{\text{max}}| = 1.4$ e Å⁻³.

Variata. Material of this compound was badly twinned and data were measured on one deconvoluted reciprocal lattice component, a hemisphere being measured in mitigation and merged ($R_{\text{int}} = 0.094$) in view of the quasi $P2_1/c$ nature of the structure; an 'orthorhombic' B -centred appearance is illusory. In the refinement, zones $hk0$, $hk13$ were refined with separate scale factors. In consequences of the above difficulties, derivative geometries should be treated with due caution.

(c) *Pyridine/propionate adduct.* C₂₀H₂₀N₂O₈Ru₂, $M = 618.5$, monoclinic, space group $P2_1/c$ (no. 14), $a = 10.890(3)$, $b = 15.706(2)$, $c = 14.390(4)$ Å, $\beta = 108.78(2)^\circ$, $V = 2330$ Å³, D_c ($Z = 4$) = 1.76 g cm⁻³, $F(000) = 1224$, μ_{Mo} = 13.4 cm⁻¹; specimen: 0.38 × 0.15 × 0.35 mm; $A^*_{\text{min,max}} = 1.21, 1.64$; $2\theta_{\text{max}} = 50^\circ$; $N = 4095$, $N_0 = 2712$; $R = 0.043$, $R_w = 0.061$; $n_v = 290$, $|\Delta\rho_{\text{max}}| = 0.89$ e Å⁻³.

Variata. A hemisphere of data was measured and merged ($R_{\text{int}} = 0.049$) in attempted mitigation of any undesirable consequences of twinning.

(d) *Pyridine/pivalate adduct.* C₂₄H₂₈N₂O₈Ru₂, $M = 674.6$, monoclinic, space group $P2_1/n$ (no. 14), $a = 12.246(3)$, $b = 13.808(2)$, $c = 16.542(4)$ Å, $\beta = 95.90(2)^\circ$, $V = 2782$ Å³, D_c ($Z = 4$) = 1.61 g cm⁻³, $F(000) = 1352$, μ_{Mo} = 11.3 cm⁻¹; $A^*_{\text{min,max}} = 1.27, 1.46$; $2\theta_{\text{max}} = 55^\circ$; $N = 6503$, $N_0 = 6148$; $R = 0.041$, $R_w = 0.067$; $n_v = 438$, $|\Delta\rho_{\text{max}}| = 0.51$ e Å⁻³.

(e) *Pyridine/benzoate adduct.* C₂₄H₂₀N₂O₈Ru₂, $M = 714.61$, monoclinic, space group $C2/c$ (no. 15), $a = 28.095(1)$, $b = 10.3742(4)$, $c = 19.3657(7)$ Å, $\beta = 102.774(1)^\circ$, $V = 5504.6(3)$ Å³, D_c ($Z = 8$) = 1.724 g cm⁻³, $F(000) = 2832$, μ_{Mo} = 11.51 cm⁻¹; $2\theta_{\text{max}} = 56.6^\circ$; $N = 6859$, $N_0 = 3875$; $R = 0.035$, $R_w = 0.027$; $n_v = 361$, $|\Delta\rho_{\text{max}}| = 0.59$ e Å⁻³.

Variata. Data were measured at 123 K on a Nonius-Kappa CCD diffractometer. Solution was achieved using the teXsan crystallographic software package.²²

CCDC reference number 186/2057.

See <http://www.rsc.org/suppdata/dt/b0/b002304n/> for crystallographic files in .cif format.

Acknowledgements

Financial assistance in the form of an APA scholarship (to C. M. K.) and grants from the Special Research Centre for Green Chemistry (ARC) and Monash Research Fund (L. S., G. B. D.) are gratefully acknowledged. We thank Dr C. M. Forsyth for experimental assistance.

References

- J. G. Bullitt and F. A. Cotton, *Inorg. Chim. Acta*, 1971, **5**, 637.
- U. Matteoli, G. Menchi, M. Bianchi and F. Piacenti, *J. Mol. Catal.*, 1991, **64**, 257.
- U. Matteoli, G. Menchi, M. Bianchi, F. Piacenti, S. Ianelli and M. Nardelli, *J. Organomet. Chem.*, 1995, **498**, 177.
- H. Schumann, J. Opitz and J. Pickardt, *J. Organomet. Chem.*, 1977, **128**, 253.
- T. A. Bright, R. A. Jones and C. M. Nunn, *J. Coord. Chem.*, 1988, **18**, 361.
- R. W. Hills, S. J. Sherlock, M. Cowie, E. Singleton and M. M. de V. Steyn, *Inorg. Chem.*, 1990, **29**, 3161.
- G. R. Crooks, B. F. G. Johnson, J. Lewis and I. G. Williams, *J. Chem. Soc. A*, 1969, 2761.

- 8 S. A. Fouda, B. C. Y. Hui and G. L. Rempel, *Inorg. Chem.*, 1978, **17**, 3213.
- 9 P. A. Anderson, G. B. Deacon, K. H. Haarmann, F. R. Keene, T. J. Meyer, D. A. Reitsma, B. W. Skelton, G. F. Strouse, N. C. Thomas, J. A. Treadway and A. H. White, *Inorg. Chem.*, 1995, **34**, 6145.
- 10 M. I. Bruce, C. M. Jensen and N. L. Jones, *Inorg. Synth.*, 1989, **26**, 259.
- 11 D. St. C. Black, G. B. Deacon and N. C. Thomas, *Aust. J. Chem.*, 1982, **35**, 2445.
- 12 See for example, R. C. Mehrotra and R. Bohra, *Metal Carboxylates*, Academic Press, New York, 1983; J. M. Percy, in *Comprehensive Organic Functional Group Transformations*, ed. S. M. Roberts, Pergamon, Oxford, vol. 1, 1995, p. 560.
- 13 A. Chyla, J. P. Lorimer, T. J. Mason, G. Smith and D. J. Watson, *J. Chem. Soc., Chem. Commun.*, 1989, 603.
- 14 G. B. Deacon, F. Huber and R. J. Phillips, *Inorg. Chim. Acta*, 1985, **104**, 41.
- 15 G. B. Deacon and R. J. Phillips, *Coord. Chem. Rev.*, 1980, **33**, 227.
- 16 C. K. Johnson, ORTEP, Report ORNL-5138, Oak Ridge National Laboratory, Oak Ridge, TN, 1976.
- 17 M. I. Bruce, B. W. Skelton, A. H. White and N. N. Zaitseva, *Aust. J. Chem.*, 1999, **52**, 621.
- 18 M. Rotem, I. Goldberg, U. Shmueli and Y. Shvo, *J. Organomet. Chem.*, 1986, **314**, 185.
- 19 J. L. Templeton, *J. Am. Chem. Soc.*, 1979, **101**, 4906.
- 20 K.-B. Shiu, S.-M. Peng and M.-C. Cheng, *J. Organomet. Chem.*, 1993, **452**, 143.
- 21 S. R. Hall, G. S. D. King and J. M. Stewart (Editors), *The Xtal 3.4 User's Manual*, University of Western Australia, Lamb, Perth, 1995.
- 22 teXsan: Crystal Structure Analysis Package, Molecular Structure Corporation, Wisconsin, MA, 1985 and 1992.
- 23 N. Walker and D. Stuart, DIFABS, *Acta Crystallogr., Sect. A*, 1983, **39**, 158.
- 24 P. T. Beurskens, G. Admiraal, G. Beurskens, W. P. Bosman, R. de Gelder, R. Israel and J. M. M. Smits, DIRDIF94, 1994.